

DIFFRACTION OF SH WAVES BY A SYSTEM OF CRACKS: SOLUTION BY AN INTEGRAL EQUATION METHOD

D. GROSS and CH. ZHANG

Institute of Mechanics, TH Darmstadt, 6100 Darmstadt, Federal Republic of Germany

(Received 17 December 1986)

Abstract—A set of straight cracks in an infinite elastic medium under time harmonic SH-wave loading is considered. Using the representation theorem for the displacements the problem is described by a system of integral equations. Numerical solutions for dynamic stress intensity factors of various crack configurations are presented and crack interaction phenomena are discussed.

1. INTRODUCTION

The dynamic mode III problem of cracks in an infinite elastic region loaded by time harmonic SH waves often has been discussed in the literature. Using integral transform techniques Loeber and Sih[1] and Mal[2] among others investigated the diffraction of an incident plane wave by a single crack. Gross[3, 4] solved the same problem for a plane and for a circular wave by means of wave function expansions. Some results can also be found in Ref. [5]. Two collinear cracks of equal length loaded by a normally incident plane wave were considered by Jain and Kanwal[6] and Itou[7]. However, it seems that on account of the mathematical complexity research has been restricted to the cases of a single crack and of two collinear cracks. To the authors' knowledge there are no analytical investigations which are applicable to general cases of two or more cracks.

In this paper the plane problem of an infinite region containing an arbitrary set of straight cracks which are excited by an incident time harmonic SH wave is investigated. Using the representation theorem for the displacements, the boundary value problem is formulated in terms of singular integral equations for the displacement jump across the cracks. An appropriate expansion of the unknown function into Chebyshev polynomials leads to a system of algebraic equations for the expansion coefficients; the latter are directly connected with the dynamic stress intensity factors. As examples various configurations of two cracks loaded by plane waves of different incident angles are considered and numerical results are presented.

2. BASIC EQUATIONS

We consider a plane infinite elastic region containing N straight cracks of length $2a_\kappa$ with $\kappa = 1, \dots, N$ (Fig. 1). The location of the κ th crack with respect to the global coor-

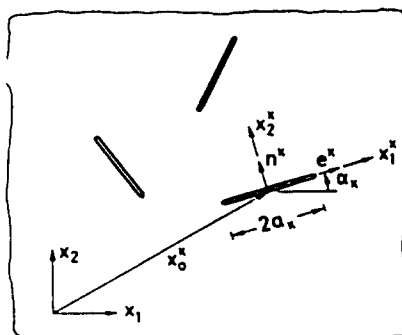


Fig. 1. Crack system in an infinite region.

ordinates x_1, x_2 can be described by the position vector \mathbf{x}_0^k of the crack centre and the crack angle α_k . With the local coordinates x_1^k, x_2^k and the accompanying unit vectors $\mathbf{n}^k, \mathbf{e}^k$ the points along the cracks are given by the position vector

$$\mathbf{x}^k = \mathbf{x}_0^k + x_1^k \mathbf{e}^k, \quad |x_1^k| \leq a_k. \quad (1)$$

The elastodynamic scattering problem of time harmonic SH waves is described by the wave equation

$$w_{,xx} + k^2 w = 0 \quad (2)$$

the constitutive relation

$$\tau_x = \mu w_{,x} \quad (3)$$

and the boundary conditions along the traction free assumed cracks

$$\tau_x(x_1^k) n_x^k = 0, \quad |x_1^k| \leq a_k, \quad \kappa = 1, \dots, N. \quad (4)$$

Herein $w(x_1, x_2)$ is the displacement in the x_3 -direction and for the only non-vanishing stress components the notation $\tau_x = \sigma_{jx}$ with $\alpha = 1, 2$ is introduced. The quantities k, μ and n_x^k are the wave number, the shear modulus and the components of the normal vector \mathbf{n}^k , respectively. Subscripts after a comma denote differentiation with respect to the corresponding coordinates, and the summation convention applies.

If an incident wave impinges on the cracks, then scattered waves are induced. The total fields of displacement w and stress τ_x can be written as a sum of the incident field w^i, τ_x^i and the scattered field w^s, τ_x^s which satisfy eqns (2) and (3) (the time factor $e^{i\omega t}$ is omitted throughout the analysis)

$$w = w^i + w^s, \quad \tau_x = \tau_x^i + \tau_x^s. \quad (5)$$

If the incident field is known, then the main task involves the determination of the scattered field. Using the representation theorem[8-10] the scattered displacement field can be expressed in the form

$$w^s(\mathbf{x}') = \sum_{\kappa=1}^N \int_{a_\kappa}^{a_\kappa} \sigma_2^s n_x^k \Psi^k d x_1 \quad (6)$$

with the Green's function

$$\sigma_2^s(\mathbf{x}^k, \mathbf{x}') = \frac{i}{4} \frac{\partial}{\partial x_2} H_0^{(1)}(k|\mathbf{x}^k - \mathbf{x}'|) \quad (7)$$

and the displacement jump across the cracks

$$\Psi^k(x_1^k) = w^s(x_1^k, 0^+) - w^s(x_1^k, 0^-). \quad (8)$$

In eqn (7) $H_0^{(1)}$ denotes the Hankel function of the first kind and zeroth order; $|\mathbf{x}^k - \mathbf{x}'|$ is the distance between the source point \mathbf{x}^k and the observation point \mathbf{x}' .

It should be pointed out, that the behaviour of Ψ at the crack tips is known. From the near field formulas[11], which are the same in the static and in the time harmonic case, it follows that for $r \rightarrow 0$

$$\Psi \rightarrow \frac{4K}{\mu\sqrt{2\pi}} \sqrt{r}. \quad (9)$$

Here r is the distance from the crack tip and K is the mode III stress intensity factor.

Introducing eqn (6) into eqn (3), boundary conditions (4) lead to the integral equations

$$\tau_{\beta}^i(x^i)n_{\beta}^i = -\mu \lim_{x' \rightarrow x^i} \frac{\partial}{\partial x_{\beta}'} \sum_{\kappa=1}^N a_{\kappa} \int_{-1}^1 \sigma_{\alpha}^{\kappa} n_{\alpha}^{\kappa} n_{\beta}^{\kappa} \Psi^{\kappa}(s) ds \quad (10)$$

for the unknown functions Ψ^{κ} , where $s = x^i/a_{\kappa}$ and $\lambda = 1, \dots, N$. The left-hand side of eqn (10) describes the known traction on account of the incident wave.

If Ψ^{κ} is determined, the total displacement and stress field can be calculated from eqns (6), (7), (3) and (5). From expression (9) we get for the stress intensity factors of the κ th crack

$$K_{\kappa}^{\pm} = \frac{\mu}{4} \sqrt{\left(\frac{2\pi}{a_{\kappa}}\right)} \lim_{s \rightarrow \pm 1} \frac{1}{\sqrt{(1 \mp s)}} \Psi^{\kappa}(s). \quad (11)$$

The plus and minus sign indicates the right and the left crack tip, respectively.

3. SOLUTION OF THE INTEGRAL EQUATION

The asymptotic behaviour of the Hankel function $H_0^{(1)}(z)$ for $z \rightarrow 0$ is given by

$$H_0^{(1)}(z) \rightarrow \frac{2i}{\pi} \ln \frac{z}{2}. \quad (12)$$

Consequently the kernel functions in eqn (10) behave as

$$\frac{\partial}{\partial x_{\beta}'} \sigma_{\alpha}^{\kappa} n_{\alpha}^{\kappa} n_{\beta}^{\kappa} \sim \frac{1}{|x^{\kappa} - x^i|^2} \quad (13)$$

as $x' \rightarrow x^i$: they are hypersingular. For the purpose of a numerical solution the integral equations therefore require a specific treatment. In this paper a Galerkin method is used.

We represent Ψ^{κ} as the series

$$\Psi^{\kappa}(s) = a_{\kappa} \sqrt{(1-s^2)} \sum_{m=1}^{\infty} C_m^{\kappa} U_{m-1}(s) \quad (14)$$

where $U_{m-1}(s)$ are Chebyshev polynomials of the second kind and C_m^{κ} are unknown expansion coefficients. This ansatz shows a behaviour at the crack tips which is in accordance with expression (9). Substituting eqn (14) into eqn (10), multiplying both sides by $\sqrt{(1-s^2)} U_{n-1}(s)$ and integrating from -1 to 1 , with the orthogonality relation of the Chebyshev polynomials we obtain an infinite system of linear algebraic equations for C_m^{κ}

$$\sum_{m=1}^{\infty} A_{mn}^{\lambda\kappa} C_m^{\kappa} = B_n^{\lambda}, \quad \kappa, \lambda = 1, \dots, N. \quad (15)$$

Coefficients $A_{mn}^{\lambda\kappa}$ and the right-hand side are given by

$$A_{mn}^{\lambda\kappa} = -\mu \int_{-1}^1 \left\{ \sqrt{(1-s^2)} U_{n-1}(s) \lim_{x' \rightarrow x^i} \sum_{\kappa=1}^N a_{\kappa}^2 \frac{\partial}{\partial x_{\beta}'} \int_{-1}^1 \sigma_{\alpha}^{\kappa} n_{\alpha}^{\kappa} n_{\beta}^{\kappa} \sqrt{(1-s^2)} U_{m-1}(s) ds \right\} ds \quad (16)$$

$$B_n^{\lambda} = \int_{-1}^1 \sqrt{(1-s^2)} U_{n-1}(s) \tau_{\beta}^i(x^i) n_{\beta}^{\lambda} ds. \quad (17)$$

The stress intensity factors are directly connected with the coefficients C_m^* . Inserting eqn (14) into eqn (11) with $U_{m-1}(\pm 1) = m(\pm 1)^{m-1}$ [13] we obtain

$$K_k^\pm = \frac{\mu}{2} \sqrt{(\pi a_k)} \sum_{m=1}^{\infty} (\pm 1)^{m-1} m C_m^*. \quad (18)$$

It is obvious that in numerical calculations m and n in eqns (14)–(18) (that is to say the number of Chebyshev polynomials taken into account) is limited. If the incident wave and the geometrical configuration of the crack system is known, then the quantities A_{mn}^* , B_n^* and consequently C_m^* can be calculated with sufficient accuracy by appropriate numerical procedures.

4. EXAMPLES

For all examples the incident wave is taken as a plane wave. It is given by

$$w^i = \hat{w} \exp [ik(x_1 \sin \theta + x_2 \cos \theta)] \quad (19)$$

where \hat{w} is the amplitude and θ is the incident angle. From eqn (4) we get for the stress amplitude of this wave $\hat{\tau} = i\mu k \hat{w}$.

As the physically most important quantities only the stress intensity factors of the cracks are considered.

4.1. The single crack

Although for the single crack results already exist in the literature, this case will be considered here once more as a test case. Equation (15) reduces to the simple form

$$\sum_{m=1}^{\infty} A_{mn} C_m = B_n. \quad (20)$$

For the crack of length $2a$ it is assumed that the local and global coordinate systems coincide. Using the Fourier integral representation of the Hankel function $H_0^{(1)}$ the matrix A_{mn} can then be written as [10]

$$A_{mn} = mn \exp \left(\frac{m+n}{2} i\pi \right) \int_{-a}^a \frac{\gamma}{\xi^2} J_m(\xi a) J_n(\xi a) d\xi \quad (21)$$

where

$$\gamma = \begin{cases} (\xi^2 - k^2)^{1/2} & \text{for } \xi \geq k \\ -i(k^2 - \xi^2)^{1/2} & \text{for } \xi < k \end{cases} \quad (22)$$

and J_m are the Bessel functions of the first kind. The right-hand side of eqn (20) becomes

$$B_n = \frac{\hat{\tau}}{\mu} \frac{4n(-1)^n}{ka} \cot \theta J_n(ka \sin \theta) \exp \left(\frac{n-1}{2} i\pi \right). \quad (23)$$

The accuracy of the calculated stress intensity factors depends on the number of expansion coefficients taken into account. Numerical calculations have shown, that for $ka \leq 8$ terms ($m, n < 11$) are sufficient to achieve an accuracy of 1%.

In Fig. 2 the dimensionless stress intensity factor $K^\pm / \hat{\tau} \sqrt{(\pi a)}$ is plotted as a function of the dimensionless wave number ka for different incident angles θ . A comparison with data of other authors shows a very good agreement. From the figure the unexpected result comes

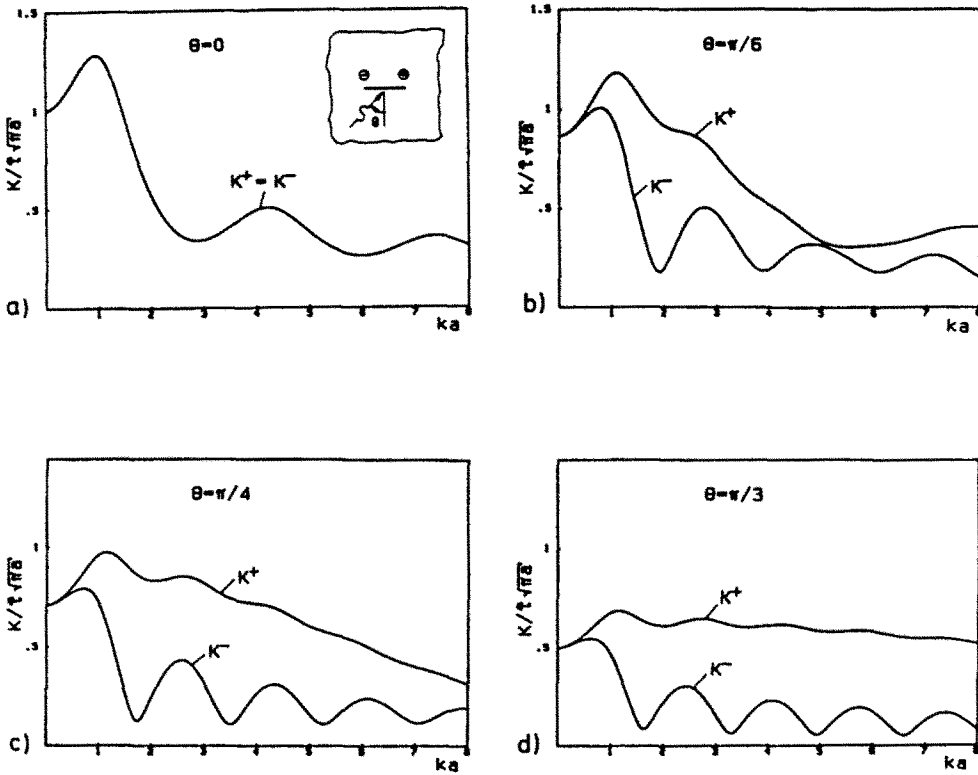


Fig. 2. K -Factors of a single crack.

out, that for $\theta = \pi/6, \pi/4, \pi/3$ the stress intensity factor at the right crack tip generally is higher than at the left tip.

4.2. Two parallel cracks

For the two parallel cracks in Fig. 3 which are loaded by the wave (19) eqn (15) can be written as

$$\sum_{m=1}^{\infty} (A_{mn}^{11}C_m^1 + A_{mn}^{12}C_m^2) = B_n^1$$

$$\sum_{m=1}^{\infty} (A_{mn}^{21}C_m^1 + A_{mn}^{22}C_m^2) = B_n^2 \tag{24}$$

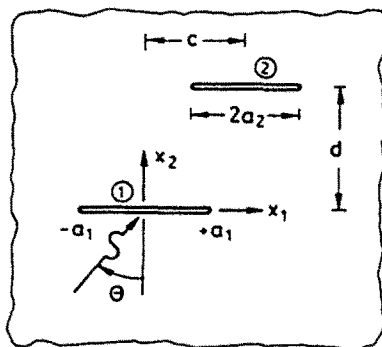


Fig. 3. Two parallel cracks.

with

$$\begin{aligned}
 A_{mn}^{11} &= mn \exp\left(\frac{m+n}{2}i\pi\right) \int_{-x}^x \frac{\gamma}{\xi^2} J_m(\xi a_1) J_n(\xi a_1) d\xi \\
 A_{mn}^{12} &= \frac{a_2}{a_1} mn \exp\left(\frac{m+n}{2}i\pi\right) \int_{-x}^x \frac{\gamma}{\xi^2} J_m(\xi a_2) J_n(\xi a_1) \exp(i\xi c - \gamma d) d\xi \\
 A_{mn}^{21} &= \frac{a_1}{a_2} mn \exp\left(\frac{n+n}{2}i\pi\right) \int_{-x}^x \frac{\gamma}{\xi^2} J_m(\xi a_1) J_n(\xi a_2) \exp(-i\xi c - \gamma d) d\xi \\
 A_{mn}^{22} &= mn \exp\left(\frac{m+n}{2}i\pi\right) \int_{-x}^x \frac{\gamma}{\xi^2} J_m(\xi a_2) J_n(\xi a_2) d\xi
 \end{aligned}
 \tag{25}$$

and

$$\begin{aligned}
 B_n^1 &= \frac{\hat{\tau}}{\mu} \frac{4n(-1)^n}{ka_1} \cot \theta J_n(ka_1 \sin \theta) \exp\left(\frac{n-1}{2}i\pi\right) \\
 B_n^2 &= \frac{\hat{\tau}}{\mu} \frac{4n(-1)^n}{ka_2} \cot \theta J_n(ka_2 \sin \theta) \exp\left[ik(c \sin \theta + d \cos \theta) + \frac{n-1}{2}i\pi\right].
 \end{aligned}
 \tag{26}$$

In contrast to A_{mn}^{11} , A_{mn}^{22} , which are always symmetric with respect to m, n the matrices A_{mn}^{12} and A_{mn}^{21} are only symmetric if the lengths of both cracks are equal. As a consequence the numerical calculations for cracks of different length are more cumbersome than for cracks of equal length.

In the following some special cases are considered. Figure 4 shows the normalized K -factors for collinear cracks. As it can be seen from Figs 4(a) and (b) for a normally incident

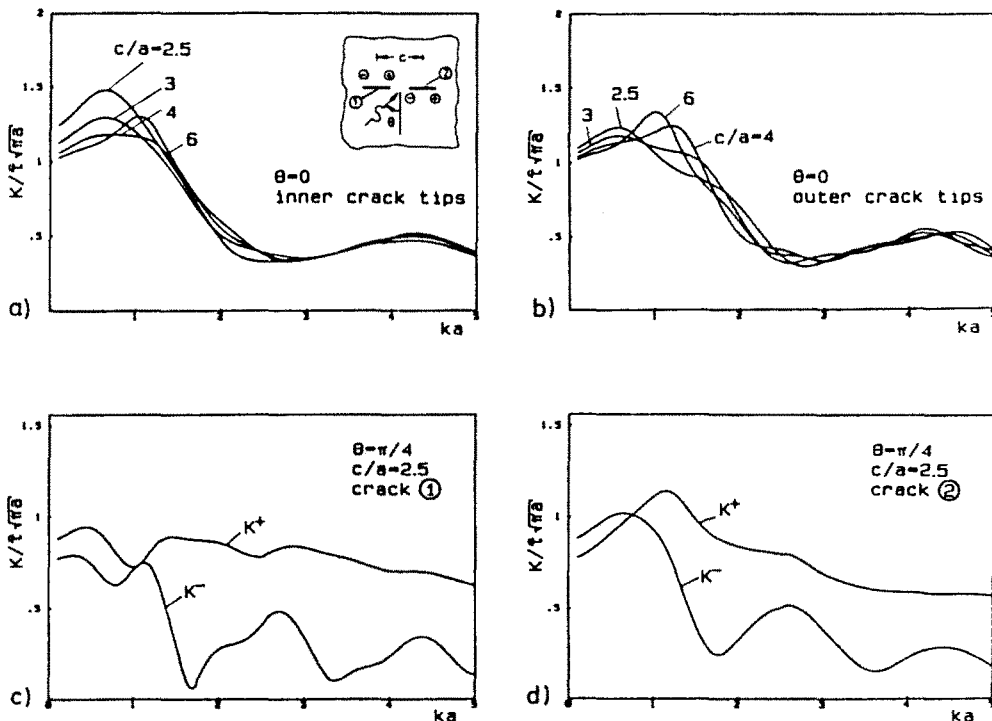


Fig. 4. K -Factors of collinear cracks of equal length.

wave the interaction depends on the distance c of the crack centres. With increasing distance the results approach that of a single crack. For the static case ($ka \rightarrow 0$) the K values of the inner tips are higher than for the outer tips. In the dynamic case the opposite may occur for a specific distance and wave number.

Results for an incident angle $\theta = \pi/4$ and $c/a = 2.5$ are plotted in Figs 4(c) and (d). Similar to the single crack K^+ lies above K^- for higher wave numbers. The differences in the results for the two cracks are due to the interaction.

In Fig. 5 collinear cracks of different lengths are considered. The influence of the left (longer) on the right (shorter) crack increases with increasing length ratio a_1/a_2 .

The results for two parallel cracks of equal length (Fig. 6) would be difficult to predict on the basis of intuitive argument. With decreasing distance the first maximum increases and is shifted to higher wave numbers. Furthermore, the maximum of the first crack is higher than for the second one. Also remarkable is the steep increase and decrease, respectively, of the curves near this maximum especially for $\theta = \pi/4$. For specific distances and wavelengths a zero (or nearly zero) K -factor may occur at a crack tip.

As a final example, a general configuration of equal cracks is considered in Fig. 7. The

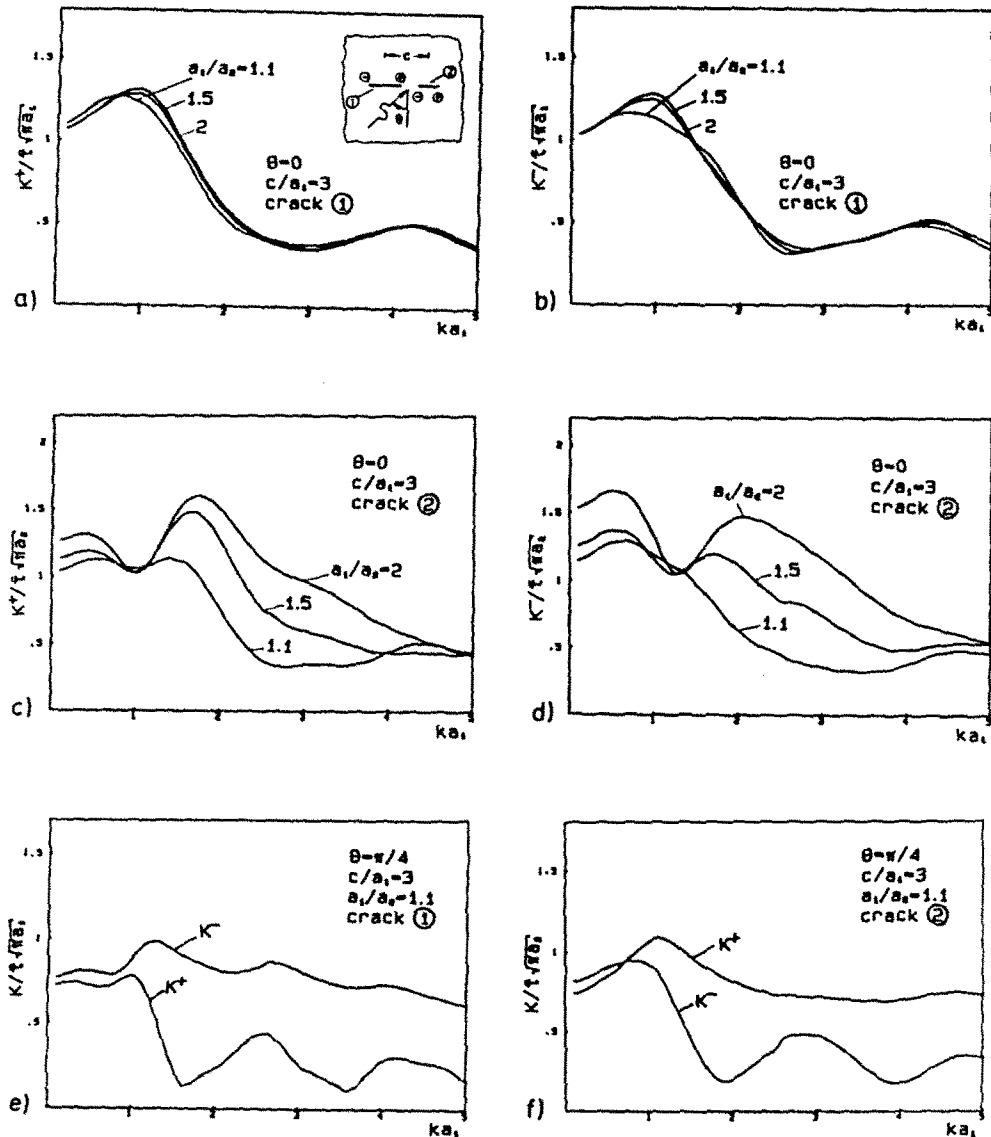


Fig. 5. K -Factors of collinear cracks of different length.

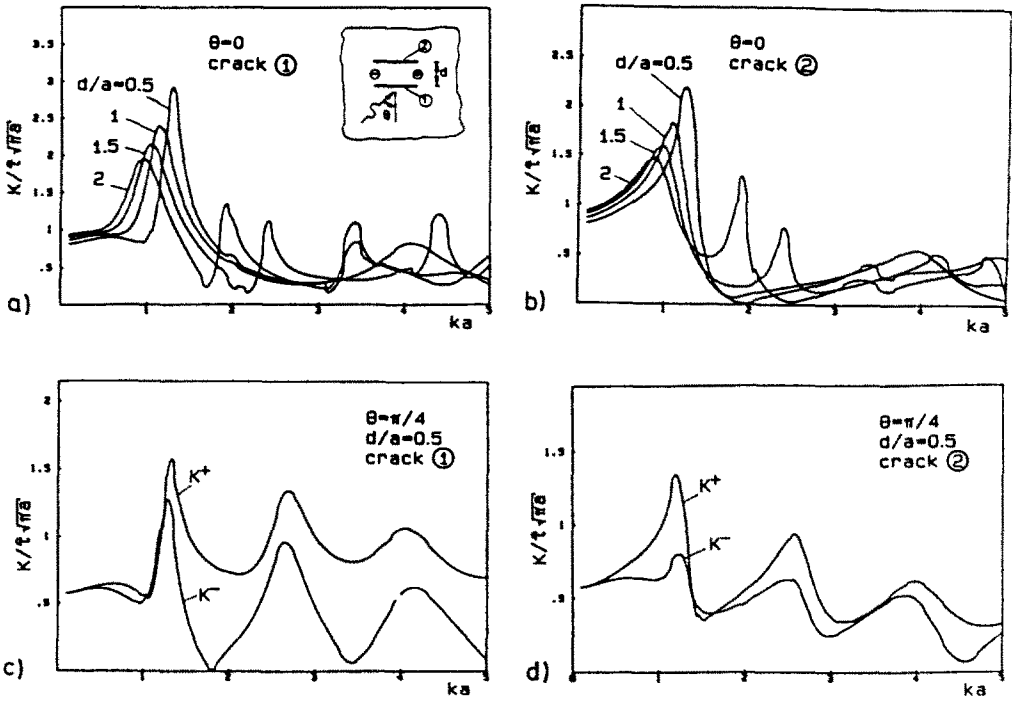


Fig. 6. K-Factors of parallel cracks.

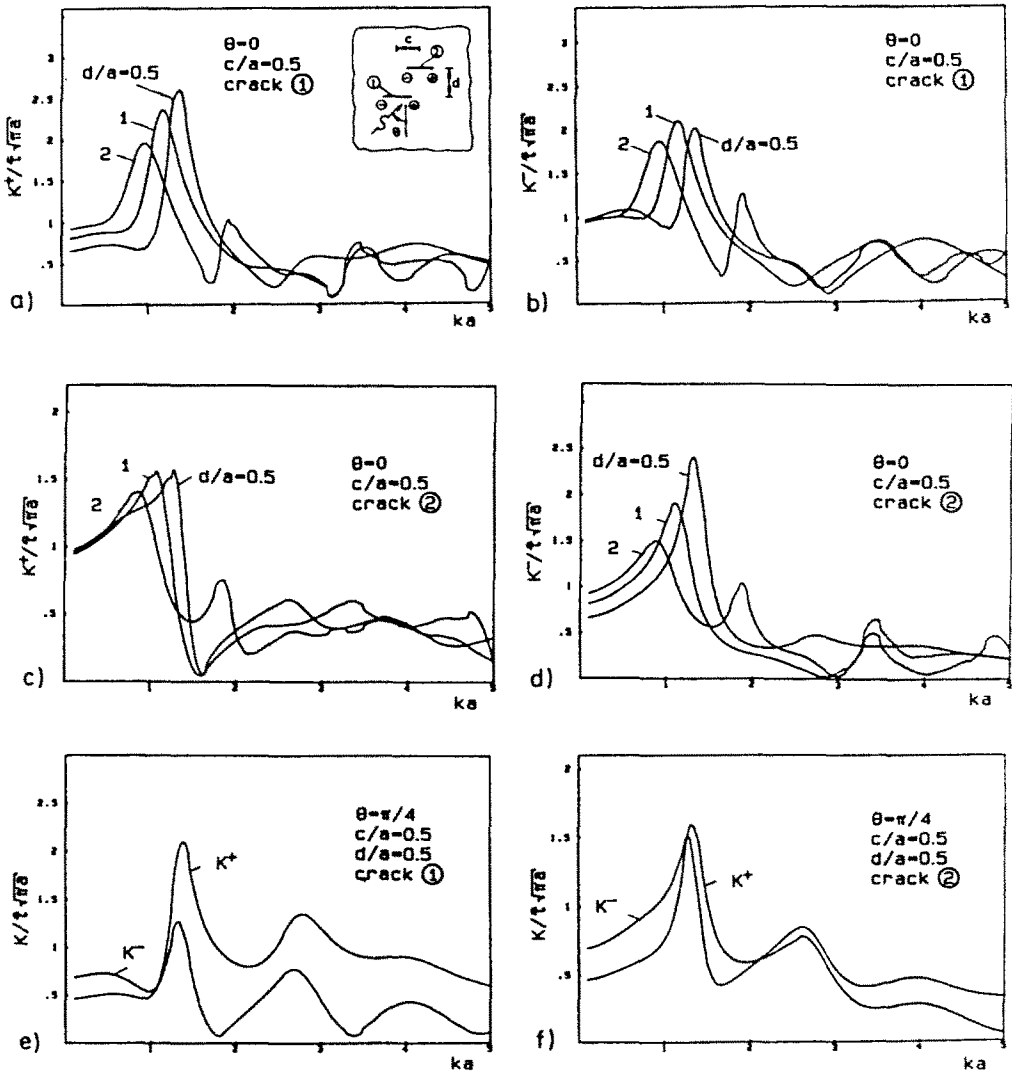


Fig. 7. K-Factors of a general configuration of parallel cracks.

interaction becomes stronger with decreasing distance of the cracks. This leads to increasing maxima of the curves but also to very low K values for certain specific parameters.

REFERENCES

1. J. F. Loeber and G. C. Sih, Diffraction of antiplane shear waves by a finite crack. *J. Acoust. Soc. Am.* **44**, 90-98 (1968).
2. A. J. Mal, Interaction of elastic waves with a Griffith crack. *Int. J. Engng Sci.* **8**, 763-776 (1970).
3. D. Gross, Dynamische Spannungskonzentration am elliptischen Loch bei Beanspruchung durch ebene SH-Wellen. *Acta Mechanica* **16**, 241-254 (1973).
4. D. Gross, Beiträge zu den dynamischen Problemen der Bruchmechanik. *Habilitationschrift*, Stuttgart (1974).
5. G. C. Sih (Editor), Elastodynamic crack problems. In *Mechanics of Fracture*, Vol. 4. Noordhoff, Leyden (1977).
6. D. L. Jain and R. P. Kanwal, Diffraction of elastic waves by two coplanar Griffith cracks in an infinite elastic medium. *Int. J. Solids Structures* **8**, 961-975 (1972).
7. S. Itou, Diffraction of an antiplane shear wave by two coplanar Griffith cracks in an infinite elastic medium. *Int. J. Solids Structures* **16**, 1147-1153 (1980).
8. J. D. Achenbach, *Wave Propagation in Elastic Solids*. North-Holland, Amsterdam (1976).
9. V. D. Kupradze, *Three-dimensional Problems of the Mathematical Theory of Elasticity and Thermoelasticity*. North-Holland, Amsterdam (1979).
10. Ch. Zhang, Die Anwendung von Integralgleichungsmethoden zur Lösung dynamischer Rißprobleme, Thesis, Technische Hochschule Darmstadt (1986).
11. H. Liebowitz (Editor), *Fracture*, Vol. 2. Academic Press, New York (1968).
12. W. Abramowitz and I. A. Stegun, *Handbook of Mathematical Functions*. Dover, New York (1965).
13. I. M. Ryzhik and I. S. Gradshteyn, *Table of Integrals, Series and Products*. Academic Press, New York (1965).